Vol. 118, No. 3, 1984 BIOCHEMICAL AND BIOPHYSICAL RESEARCH COMMUNICATIONS
February 14, 1984 Pages 885-893

DISPERSITY OF DES-L•VAL^7-D•VAL^8-GRAMICIDIN A SINGLE CHANNEL CONDUCTANCES ARGUES FOR DIFFERENT SIDE CHAIN ORIENTATIONS AS BASIS

D. W. Urry, S. Alonso-Romanowski, C. M. Venkatachalam, R. D. Harris and K. U. Prasad

Laboratory of Molecular Biophysics,
University of Alabama in Birmingham,
School of Medicine, Birmingham, Alabama 35294

Received December 20, 1983

Planar bilayer studies are reported on the channel activity of des-L•Val^7-D•Val^8-Gramicidin A. This analog is designed to provide more long-lived side chain distributions involving the Trp residues than occur with Gramicidin A. The carbonyls of these residues coordinate the permeant cation and the energetics of the coordination, which is proposed to depend on side chain orientation, determines the free energies of the rate limiting entrance-exit barriers and the binding sites. The finding of an increased dispersity of single channel conductance for the analog supports the perspective that dispersity derives from different side chain distributions on the same backbone conformation. Channel mechanism is not understood until dispersity is explained.

Gramicidin A, HCO-L•Val^1-Gly^2-L•Ala^3-D•Leu^4-L•Ala^5-D•Val^6-L•Val^7-D•Val^8-L•Trp^9-D•Leu^{10}-L•Trp^{11}- D•Leu^{12}-L•Trp^{13}-D•Leu^{14}-L•Trp^{15}-NHCH$_2$CH$_2$OH (1), forms monovalent cation selective channels in planar bilayer membranes. The cation current passing through a single Gramicidin A channel is generally constant over the lifetime of the channel, but the observed single channel currents are not confined to a single narrow range of values (2). The data is represented as a histogram of the frequency of occurrence as a function of single channel conductance. In diphytanoyl lecithin (DPhL) membranes at 30°C, approximately 60% of Gramicidin A (GA) channel events fall within the most probable distribution near the upper edge of the conductance range when added to the bath at a concentration in methanol to result in picomolar concentrations. The other 40% of channel events exhibit lesser conductance and are spread over a wide range of values (see GA comparative curve in Figure 3 below). This dispersity of single channel conductances (or currents) is not due to different analogs of the natural Gramicidin mixture as high pressure liquid chromatographically

0006-291X/84 $1.50

pure GA and synthetic GA give essentially identical histograms (3). Also synthetic Gramicidin C (Tyr^{11}-GA) synthetic Gramicidin B (Phe^{11}-GA) and synthetic Phe^{9}-GA show the dispersity (4-6). This dispersity is not due to a mixture of dimers of single stranded β-helices (7,8) and of double stranded β-helices (9) as the data both on planar bilayer conductance studies (10,11) and on channels in membrane suspensions (12,13) argue strongly that greater than 90% of the channel states are the head to head dimerized single stranded β-helical conformation; different combinations of end to end dimerizations are similarly not responsible (10-13). Structures with different numbers of residues per turn (7) could possibly contribute but it is hard to explain similar selectivities and channel lifetimes and these three or four possibilities could not explain the extent of the diversity. Indeed there is even dispersity within the most probable conducting state. Interestingly, it has been shown that a channel can change its conducting state without turning "off" and back "on" (14).

The proposal has been made that different side chain distributions are responsible for the observed dispersity (15) with the argument that the energy of peptide carbonyl libration into the channel to effect the necessary ion coordination depends on orientation of side chain. This argument would require that different side chain distributions could have lifetimes as long as seconds. Our approach to the question is to develop analogs with markedly different distributions of states that reasonably follow from the possible side chain orientations of the analogs. It would, of course, be strong support of this perspective if analogs could be designed based on an analysis of side chain distributions in which one would increase the dispersity of single channel conductance whereas another would decrease the dispersity. In this report is given results on a synthetic analog that increases dispersity.

MATERIALS AND METHODS

The synthesis of the des-L·Val^{7}-D·Val^{8}-GA analog was carried out by the solid phase method of peptide synthesis as described previously (5,6). A formyl group was used for the β-indole ring protection to suppress any destruction of Trp residues during the acid deprotection steps. The Boc-peptide was

cleaved from the resin by ethanolamine treatment which simultaneously removed the N^{indole}-formyl protecting group. After the Boc-group was removed, the Gramicidin analog was formylated and purified. The details will be published elsewhere. In addition to the usual peptide chemistry methods, the synthesis was verified and the purity demonstrated by both carbon-13 and proton nuclear magnetic resonance (NMR) as shown by the latter in Figure 1 for a comparison

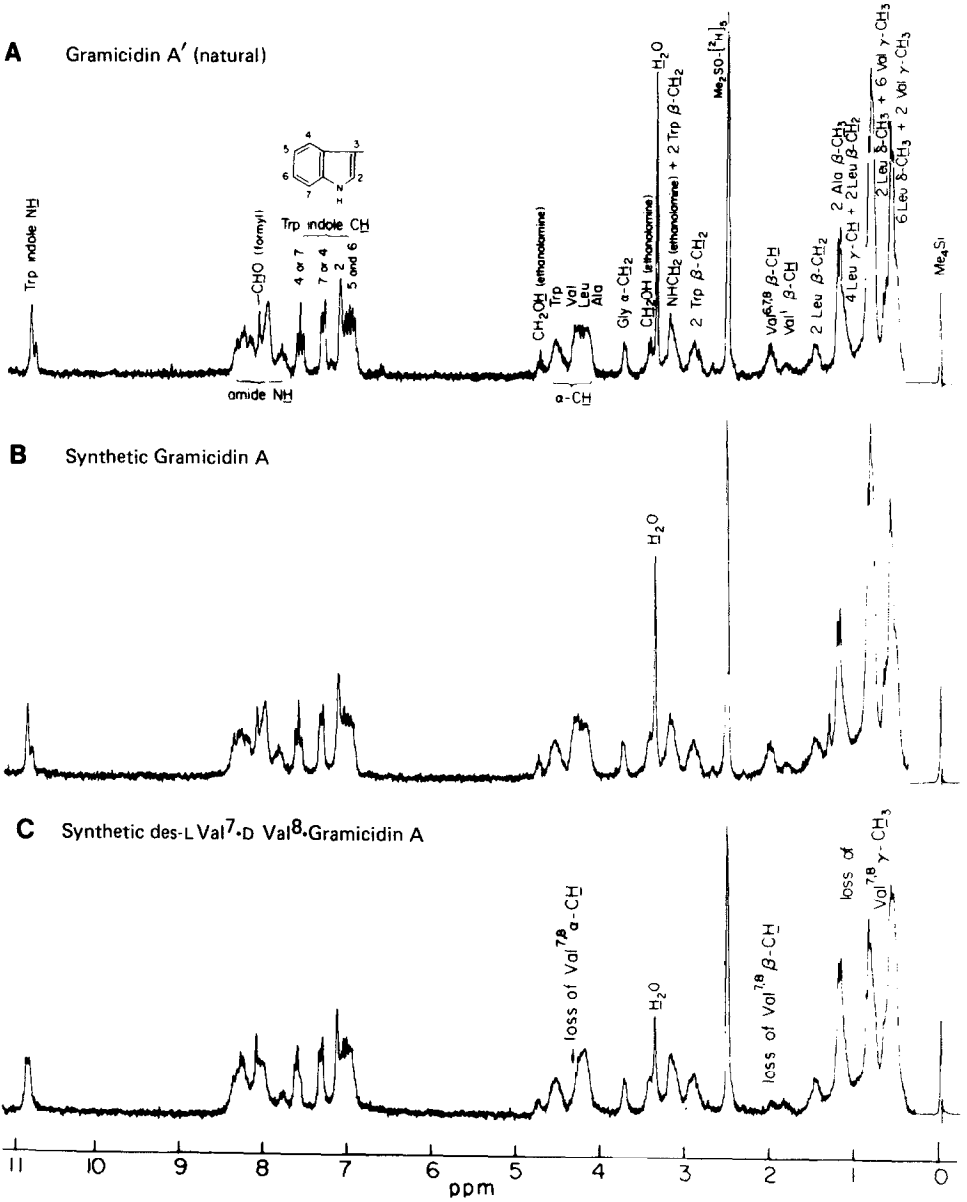

FIGURE 1: Proton magnetic resonance spectra at 220 MHz and 20°C in dimethyl-d_6-sulfoxide. A. commercially available Gramicidin which is the mixture seen in Figure 2A. B. synthetic Gramicidin A. C. synthetic des-L·Val^7-D·Val^8-GA. Note the loss of the Val αCH, βCH and γCH_3 resonances, the retention of the other reasonances and the absence of extraneous peaks. Note also that the four indole NH resonances near 11 ppm split 2:2 for the analog rather than 3:1 for GA.

with the natural Gramicidin mixture. Having demonstrated by NMR that the product purity is greater than 95%, des-L•Val^{7}-D•Val^{8}-GA was passed through an analytical high pressure liquid chromatography (HPLC) column where the major peak is clearly the desired analog (see Fig. 2). The peak is collected, passed several more times through the analytical HPLC column and in the final pass a fraction is collected for the planar bilayer studies. This assures the highest purity for the analog.

Planar black lipid membranes were formed in a hole in a Teflon partition separating two Teflon chambers each containing 7 ml of unbuffered 1 M KCl solution (16). Initially, the cell was taken apart, boiled in concentrated NaOH solution and rinsed many times with deionized, glass distilled water, with acetone, then chloroform and finally ether. Diphytanoyl lecithin (DPhL, Avanti Polar Lipids, Birmingham, AL) in n-decane (2%,w/v) was used as the membrane forming solution. When the membrane failed to form or if channel activity were too high, the cell was cleaned by means of several rinsings with water, followed by ethanol and then chloroform:methanol (2:1,v/v). The area of the black lipid membrane was approximately 0.3 mm^{2} in all cases. The temperature was maintained at 31.6±1.0°C by means of a Peltier cell (17). After the membrane was made, des-L•Val^{7}-D•Val^{8}-GA or GA was added in methanolic solution to give picomolar concentrations in the cell. The data collection

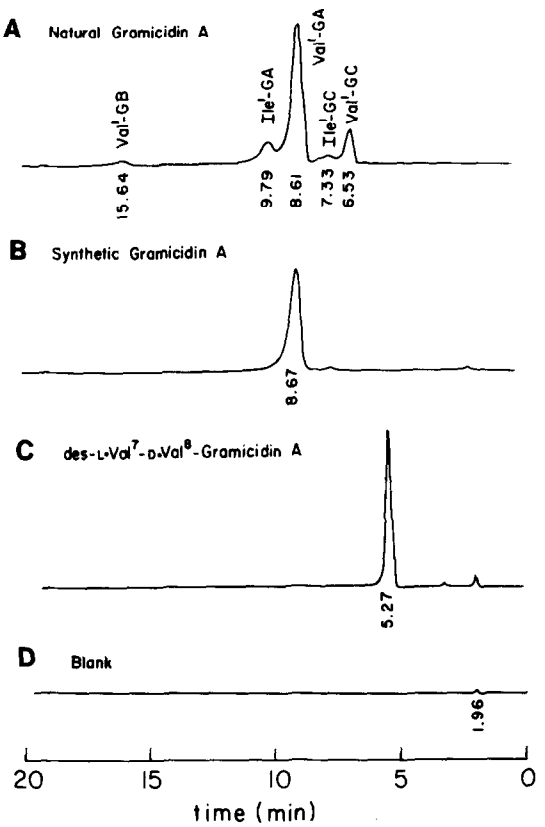

FIGURE 2: High performance liquid chromatograms A. natural Gramicidin which is a mixture of several analogs as labelled. GA is defined in the Introduction, GB = L•Phe^{11}-GA and GC = L•Tyr^{11}-GA. The other variations occur in position 1. About 70% is GA also referred to as Val^{1}-GA. B. synthetic GA used in the planar bilayer studies C. synthetic des-L•Val^{7}-D•Val^{8}-GA. D. blank.

began after achieving membrane stability and a reasonably constant single channel activity (≈1 hour). The electrical measurements were made with Ag-AgCl electrodes and the applied voltage clamp was 100 mV. All the events used to develop the histogram were collected from the same membrane. The cell and voltage source are contained in a small shielded box mounted upon a vibration free air-isolated Micro-g table. The signal from the cell was fed into an Analog Devices Model 52K operational amplifier with 250 mV/μsec minimum slew rate and then filtered by a Krohn-Hite dual filter Model 3342 used in the low pass RC mode, 200 Hz and 20 dB gain (using both filters connected in series).

The digitized conductance data, recorded on the storage oscilloscope of a Nicolet Model 2090, were transferred to the Tektronix 4054A computer through an RS-232 interface. The analysis of the data in the computer was done in two stages. In the first stage, each conductance sweep, consisting of 4096 conductance values, was processed by a transition-detection algorithm to pick out the time of occurrence and the conductance height of all the transitions occurring within the time window of the sweep. This algorithm is based on a rapid determination of the points where the derivative of the signal exceeded a chosen threshold value. An "idealized" delineation of the signal is achieved in this stage in terms of the recognized transitions. In the second stage, the single channel events occuring in each sweep were characterized as to their conductance and lifetime by optimally matching the downward transitions with their corresponding upward transitions. The method of analysis is more fully discussed elsewhere (17).

RESULTS AND DISCUSSION

As shown in Figure 3, the histogram of the single channel conductances for the des-L·Val^{7}-D·Val^{8}-GA analog shows a very broad peak covering a 20 picoSiemen (pS) range from 5 pS to 25 pS and centered near 17 pS. On the other hand, the most probable conductance peak for GA, obtained under similar conditions, covers a 4 pS range centered near 26 pS. This marked spreading was anticipated from conformational analysis of side chains (15) and in a first order consideration is explicable in terms of the differences in the Trp side chain distributions. In this regard, it is important to realize that the peptide carbonyls of the Trp residues provide direct lateral coordination of the cation at the rate limiting entrance-exit barrier (18,19) and at the binding site (20,21), and it is the energetics for peptide libration, which is required to achieve ion coordination and which is proposed to depend on side chain orientation, that determines the free energies of the barriers and binding sites (15).

As is apparent on analysis of Figure 4 for GA and as has been analyzed in greater detail elsewhere (15,22), the Trp^{11} side chain has the most freedom to assume different orientations. The Trp^{9} is most restrained in this confor-

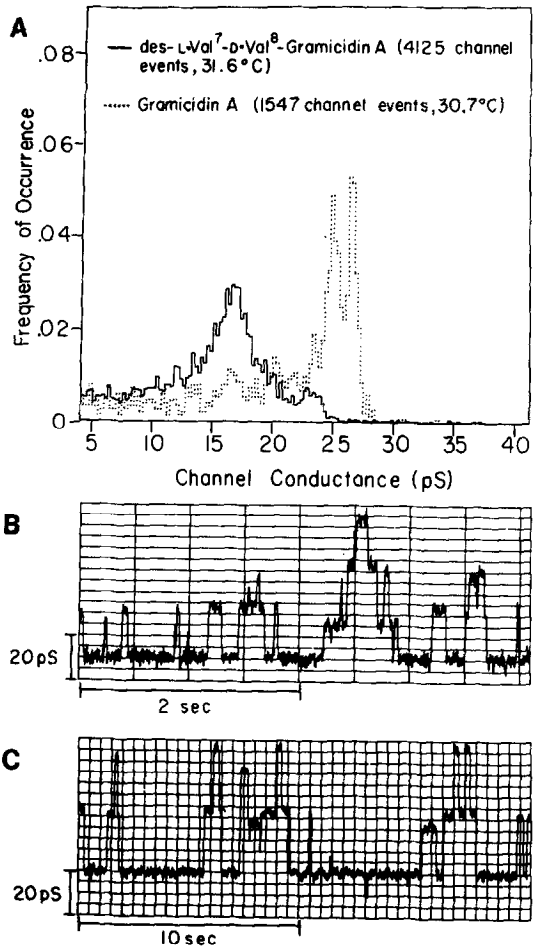

FIGURE 3: A. Single channel conductance histograms for synthetic des-L•Val^{7}-D•Val^{8} Gramicidin A (solid line) and for synthetic Gramicidin A (dotted line). These histograms have been developed in the computer. The algorithm employed detects the various conductance jumps in each sweep and then optimally matches the downward transitions with their corresponding upward transitions. The conductance cell width is 0.25 pS. While the number of events are fewer for GA the same result has been obtained many times near this temperature on DPhL membranes and using different amplifiers. The large number of events for the analog were obtained on a single membrane and is more than enough to establish the statistical significance. The same result has also been obtained using a Keithley amplifier. B. An example of an actual conductance trace recorded for synthetic des-L•Val^{7}-D•Val^{8}-Gramicidin A at 31.6°C. The sweep is composed of 4096 conductance values collected at the rate of 1 msec per point providing a time window of 4.095 secs. C. A conductance trace for synthetic Gramicidin A at 30.7°C. A 5 msec/point sampling rate has been employed spanning a window of 20.475 secs.

mation with its indole laying over the Ala^{3} side chain on one side and with the Trp^{15} indole sandwiched against it on the other side. These interactions exemplify the important i±6 side chain interactions of residue i. Whether or

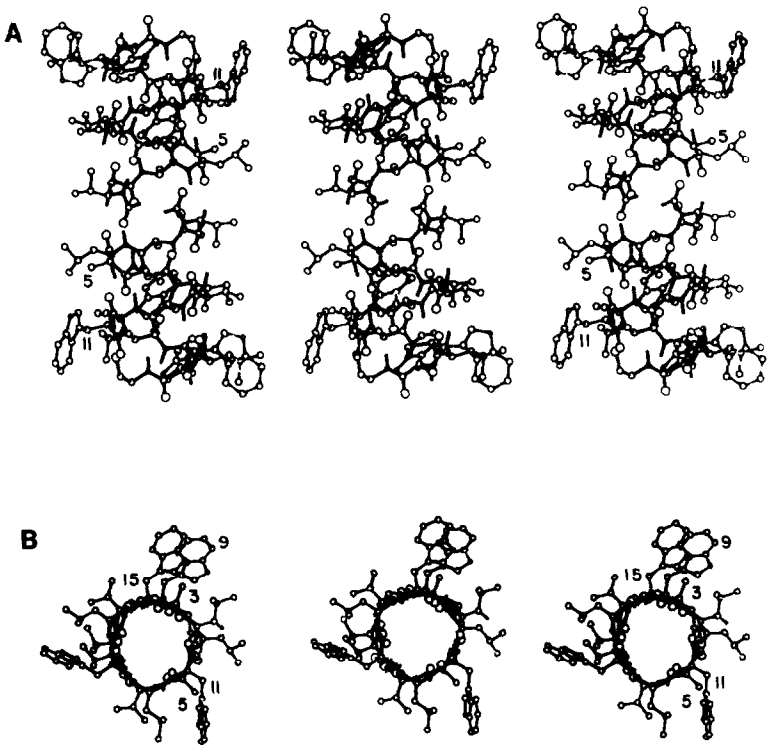

FIGURE 4: Stereo views of the in vacuo most energetically favorable conformation of the Gramicidin A transmembrane channel. It should be appreciated that this is one of many energetically similar conformations which differ in terms of the orientations of side chains. Three views are plotted in order to allow for either near (cross-eye) or distance (wall-eye) viewing. For wall-eye viewing place a piece of paper over the left hand structure and merge the right hand pair. For cross-eye viewing, cover the right hand structure and use the left hand pair. Note in particular in B (the channel view) the orientation of the Trp^{9} and Trp^{15} indoles, in both views, the similar orientations of the Trp^{11} and Trp^{13} side chains and that the Trp^{11} side chain could orient like that of Trp^{9}. Reproduced with permission from reference 22.

not a side chain can change its orientation depends also on its interactions with residues i±1 and it is the simultaneous, coordinated movement of several side chains required for a single side chain to change its rotameric state that makes the process slow. The Trp^{13} side chain is inhibited from assuming the orientation of the Trp^{9} side chain because the Val^{7} side chain is bulkier than the Ala^{3} side chain. A means of providing as much freedom for Trp^{13} as for Trp^{11} is to have the des-L•Val^{7}-D•Val^{8}-GA analog in which case the residues i-6 from the L•Trp^{11} and the L•Trp^{13} residues are the L•Ala^{3} and L•Ala^{5} residues, respectively. This is depicted in Fig. 5 which schematically shows the i±6 interactions for GA and for des-L•Val^{7}-D•Val^{8}-GA. Thus in the analog

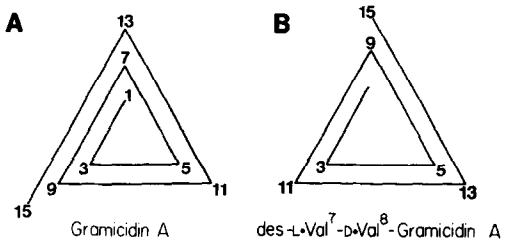

FIGURE 5: Schematic representation to identify the i ••• i±6 relationships between L-residue side chains. A. Gramicidin A which should be compared with Figure 4. B. des-L•Val^{7}-D•Val^{8}-GA which shows that Trp residues 11 and 13 pair with Ala residues 3 and 5, respectively. This allows for more combinations of side chain orientations involving the Trp residues which are at the entrance-exit barriers and binding sites.

both the side chains of L•Trp^{11} and L•Trp^{13} have freedom equivalent to the L•Trp^{11} of GA and the analog would be expected on the basis of side chain distribution affecting dispersity of single channel conductance to have a greater dispersity of single channel conductances as reported in Figure 3.

Accordingly, by making an analog in which the L•Trp^{13} side chain has as much positional freedom as the L•Trp^{11} side chain, an analog has been designed which gives an increased dispersity of single channel currents. Continuing with this perspective, it should be possible to go in the opposite direction, i.e., to design an analog with decreased dispersity of single channel currents. Using the same line of reasoning an analog which selectively decreased the positional freedom of the L•Trp^{11} side chain should decrease dispersity of single channel conductances. This should occur with the L•Leu^{5}-GA analog which has been synthesized and for which preliminary data show a sharp most probable peak in which 68% of the events occur within a single peak of 1.75 pS width whereas a comparable value for Gramicidin A would be 49%. Thus, a strong case is developing for understanding this important aspect of the Gramicidin A channel conductance. Clearly a process, in which 40% of the events and even the finite breadth of the other 60% are unexplained, is not an adequately understood process.

ACKNOWLEDGMENT

This work was supported in part by the National Institutes of Health Grant No. GM-26898. The authors wish to thank T. L. Trapane for assistance on obtaining Figure 1.

REFERENCES

1. Sarges, R., and Witkop, B. (1964) J Am. Chem. Soc. 86, 1862-1863.
2. Hladky, S. B., and Haydon, D. A. (1972) Biochim. Biophys. Acta 274, 294-312.
3. Prasad, K. U., Trapane, T. L., Busath, D., Szabo, G., and Urry, D. W. (1982) Int. J. Pept. Protein Res. 19, 162-171.
4. Bamberg, E., Noda, K., Gross, E., and Läuger, P. (1976) Biochim. Biophys. Acta 419, 223-228.
5. Prasad, K. U., Trapane, T. L., Busath, D., Szabo, G., and Urry, D. W. (1982) J. Protein Chem. 1, 191-202.
6. Prasad, K. U., Trapane, T. L, Busath, D., Szabo, G., and Urry, D. W. (1983) Int. J. Pept. Protein Res. 22, 341-347.
7. Urry, D. W., Goodall, M. C., Glickson, J. D., and Mayers, D. F. (1971) Proc. Natl. Acad. Sci. USA 68, 1907-1911.
8. Urry, D. W. (1973) Conformation of Biological Molecules and Polymers - The Jerusalem Symposia on Quantum Chemistry and Biochemistry, pp. 723-736, Israel Academy of Sciences, Jerusalem.
9. Veatch, W. R., Fossel, E. T., and Blout, E. R. (1974) Biochemistry 13, 5249-5264.
10. Apell, H.-J., Bamberg, E., Alpes, H. and Läuger, P. (1977) J. Membrane Biol. 31, 171-188.
11. Bamberg, E., H.-J. Apell, and H.. Alpes (1977) Proc. Natl. Acad. Sci. USA 74, 2402-2406.
12. Weinstein, S., Wallace, B. a., Blout, E. R., Morow, J. S., and Veatch, W. (1979) Proc. Natl. Acad. Sci. USA, 76, 4230-4234.
13. Urry, D. W., Trapane, T. L. and Prasad, K. U. (1983) Science 221, 1064-1067.
14. Busath, D., and Szabo, G. (1981) Nature 294, 371-373.
15. Urry, D. W., Venkatachalam, C. M., Prasad, K. U., Bradley, R. J., Parenti-Castelli and Lenaz, G. (1981) Int. J. Quantum Chem.:Quantum Biology Symp. No. 8, 385-399.
16. Bradley, R. J., Romine, W. O., Long, M. M., Ohnishi, T., Jacobs, M. A. and Urry, D. W. (1977) Arch. Biochem. Biophys. 178, 468-474.
17. Urry, D. W., Alonso-Romanowski, S., Venkatachalam, C. M., Bradley, R. J., and R. D. Harris (in preparation).
18. Urry, D. W., Venkatachalam, C. M., Spisni, A., Läuger, P. and Khaled, M. A. (1980) Proc. Natl. Acad. Sci. USA, 77, 2028-2032.
19. Finkelstein, A., and Andersen, O. S. (1981) J. Membrane Biol. 59, 155-171.
20. Urry, D. W., Prasad, K. U. and Trapane, T. L. (1982) Proc. Natl. Acad. Sci. USA, 79, 390-394.
21. Urry, D. W., Walker, J. T. and Trapane, T. L. (1982) J. Membrane Biol. 69, 225-231.
22. Venkatachalam, C. M., and Urry, D. W. (1983) J. Comput. Ch. 4, 461-469.